LASER FORMATION OF RELATIVISTIC ELECTRON MIRRORS AND GENERATION OF INCOHERENT X-RAYS

© 2025 V. V. Kulagin[a,*], V. N. Kornienko[b], V. A. Cherepenin[b]

[a]*Lomonosov Moscow State University, Sternberg State Astronomical Institute, Moscow, Russia*

[b]*Kotelnikov Institute of Radioengineering and Electronics of the Russian Academy of Sciences, Moscow, Russia*

**e-mail: victorvkulagin@yandex.ru*

Received September 06, 2024

Revised September 16, 2024

Accepted September 30, 2024

Abstract. Using numerical 2D-PIC simulations, the generation of X-rays during the interaction of an oncoming laser wave with a relativistic electron mirror formed by a powerful accelerating laser pulse from a plasma layer is investigated. The structure of the radiated field in the far zone is investigated, the spectral density of the radiation field and the angular distribution of the pulse energy are found. Changing the parameters of the accelerating and counter waves allows one to control the characteristics of the radiation.

Keywords: *generation of incoherent X-ray pulses, superintense nonadiabatic laser pulses, relativistic electron mirrors*

DOI: 10.31857/S03676765250108e5

INTRODUCTION

At present, X-rays are one of the most effective tools for studying various systems in many fields of science and technology. X-ray sources based on synchrotron radiation of relativistic electrons occupy a special place [1]. The method of X-ray generation using synchrotron radiation attracts more and more attention of researchers, which is associated with the wide spread of multiterawatt lasers and the possibility of creating on their basis an all-optical source of X-ray radiation with controlled parameters.

A synchrotron X-ray generator can be based on a laser source forming a relativistic electron mirror, whose parameters largely determine the parameters of X-ray pulses. For nanofilm, the idea of synchronous acceleration of electrons by a superpower non-adiabatic laser pulse was first proposed in [2], and then the characteristics of the formed relativistic electron mirrors were investigated [3]. At perpendicular incidence of a laser pulse with a steep front and relativistic amplitude on a plasma layer, a simultaneous displacement of all electrons of the layer along the normal to the surface under the action of the longitudinal component of the Lorentz force can occur. If the field amplitude is large enough, this force accelerates the electrons to relativistic velocities and forms a relativistic electron mirror with a diameter of the order of the laser pulse diameter and a thickness of several nanometers. Such a clot can be formed at the dimensionless amplitude of the laser pulse a_0 , exceeding a certain threshold depending on the parameters of the plasma layer [3] ($a_0 = |e|E_0/(mc\omega)$, where e and m are the charge and mass of the electron, E_0 and ω

are the amplitude and frequency of the laser with wavelengthλ and periodT_0 *, c is the* speed of light in vacuum).

At reflection of an oncoming laser pulse from a relativistic electron mirror, the frequency of the resulting electromagnetic pulse increases due to the Doppler transform. In this case, coherent radiation is formed, the characteristics of which are studied in [4,5] for perpendicular incidence of the oncoming pulse on the mirror. For coherent reflected radiation, the frequency conversion is proportional to the normalized electron energyγ , which is due to the presence of not only longitudinal motion of the mirror, but also transverse motion, as a result of which the direction of the reflected wave does not coincide with the direction of electron velocity. In addition, in the generated radiation there is also an incoherent part, for which the direction of propagation of the intensity maximum coincides with the direction of electron velocity, and the frequency conversion is proportional toγ^2 . It should be noted that such radiation can be regarded as synchrotron radiation in the field of the laser ondulator counter wave or as Thomson scattering of the counter wave by the mirror electrons in the field of the accelerating wave and the Coulomb field of the target ions, which determines the specificity of the interaction. Analytical estimates of the parameters of this radiation have shown [6] that the generation of attosecond X-ray and gamma beams with high brightness and maximum energy in MeV units is possible with modern multiterawatt lasers.

The formation of electron clots during the interaction of a high-power laser pulse with solid-state targets and the accompanying generation of incoherent X-ray and gamma radiation are widely studied in the literature [1,6-11]. Films [6-8], filaments and rods [9], strips [10], clusters [11], etc. with micrometer or nanometer dimensions along one or more directions are considered as targets. Thus, nanometer-thick films can be formed from various materials, in particular, graphene, which has been used in laser-plasma experiments for more than a decade. Both the emission of electrons in a single wave field [7,8,10,11] and the interaction with the fields of two counter waves [6,9] are considered. From the point of view of applications, the realization of the scheme with a single laser pulse is much simpler than the scheme of counter propagation of two pulses obtained from a single laser source. At the same time, the scheme with two pulses allows to provide full control of the parameters of the generated radiation, including angular distribution, photon energy, frequency integral energy in the pulse, spectral characteristics, etc., which can be essential in various applications.

The purpose of this paper is to numerically investigate the processes of formation of a relativistic electron mirror and its interaction with a counter wave, as well as to determine the characteristics of the generated incoherent radiation of the X-ray frequency range.

FORMATION OF A RELATIVISTIC ELECTRON MIRROR AND ITS INTERACTION WITH A COUNTER WAVE

To find the characteristics of the relativistic electron mirror, a computational experiment including two-dimensional (2D) numerical simulations using PIC (in English-language literature "particle-in-cell", "cloud-in-cell") codes of the process of interaction of an accelerating non-adiabatic laser pulse of relativistic amplitude with the plasma layer was carried out. The accelerating laser pulse with amplitude $a_0 = 10$, linear polarization along the *x-axis,* Gaussian transverse profile with a diameter of 20 μm (here and below the laser pulse diameter corresponds to the laser beam diameter determined by the field level e^{-1} from the maximum field value on the axis) propagates along the line x=20λ in the positive direction of the *z-axis*, wavelength $\lambda = 1$ μm. Such parameters correspond to currently widespread laser installations with pulse power of the order of 100-200 TW. The pulse has the form of a sinusoidal segment with a length of 5λ , which corresponds to a non-adiabatic form (already the first half-cycle has an amplitude close to the maximum amplitude of the pulse [4]). The thickness of the plasma layer is 5 nm and the electron concentration is 0.6-10^{22}cm^{-3}, its initial position $z = 0.5\lambda$. Characteristics of the relativistic mirror electrons after 4.5 periods T_0 of the laser field after the beginning of modeling are presented in Fig. 1.

It follows from Fig. *1a* that at the chosen parameters of the laser pulse and the target, a relativistic electron mirror is formed by the time 4.5 period T_0 of the laser field from the beginning of modeling. Electrons near the laser pulse axis (the mirror section from x=15λ to x=25λ) have the highest energy; their longitudinal momentum is significantly larger than the transverse momentum (Fig. *1b* and *1c*), and the scatter of the velocity direction does not exceed 0.2 deg. The thickness of the mirror near the laser axis is of the order of 3 nm.

The characteristics of the most energetic mirror electrons as a function of time are presented in Fig. 2. The maximum energy of the relativistic mirror electrons can reach the value $\gamma_{max} = 2a_0^2 = 200$ at the chosen target parameters [3,4], so the acceleration of the mirror electrons during the interaction with the counterwave is still ongoing (modeling of longer acceleration times requires a substantial increase in computational resources). The impulses and energies of the electrons are increasing, in particular, the energy increase is fromγ =44.5 toγ =59. The angle made by the velocity vector of the most energetic electrons of the relativistic mirror relative to the z-axis also changes from -12 to -10.5 degrees. Based on these values, it is necessary to choose the angle of incidence of the counter wave when performing computational experiments. Since the energy of electrons and the angle of their velocity vector change coherently and regularly during the interaction with the oncoming wave, the characteristics of the generated radiation (pulse energy, spectral density of radiation, etc.) will depend not only on the direction but also on time.

The counter wave in the computational experiment was set as an external field, which simplified the modification of the already available numerical code for the case of noncollinear incidence of the accelerating and counter pulses. The short duration of the counter wave allowed us to study in detail the generation of synchrotron radiation at different time moments. The geometry of the interaction of the relativistic electron mirror with the counter wave (blue bar) at the time $4.5T_0$ from the beginning of the simulation is shown in Fig. *2c*. The interaction of the mirror electrons with the counter wave begins only after the mirror has formed and the electrons have gained the required energy (in this case, the energy of the mirror electrons is approximately 4 times less than the energyγ_{max} , achievable with increasing acceleration time). A plane counter wave polarized along the *y-axis* with amplitude$a_1 = 1$ included one period of the laser fieldT_0 . Its angle of incidence was 170.3° to the *z-axis* (in Fig. *2c* the scales along the z and x axes are different). The use of different polarizations of the accelerating and counter waves allowed us to isolate the synchrotron emission of the mirror electrons associated only with the counter wave field. In this case, the radiation caused by the initial acceleration of electrons and their continued motion in the field of the accelerating wave had polarization along the *x-axis* and did not interfere with it. The duration of interaction of the counter wave with the most energetic electrons of the mirror is about $1.5T_0$ (from $3.5T_0$ to $5T_0$ after the beginning of the simulation), and it is for this time interval that the electron parameters are presented in Figs. *2a* and *2b*. The other electrons in the simulation window have significantly lower energies during the interaction with the counter wave and form the low-frequency part of the radiation, so they are not taken into account in the calculation of the far-field.

RADIATION OF MIRROR ELECTRONS WHEN MOVING IN THE COUNTER WAVE FIELD

Modeling the interaction of a laser pulse with electrons using PIC codes does not allow us to directly study the fields of X-ray and gamma frequencies. At the same time, their generation occurs as a result of motion and synchrotron emission of electrons in the field of an oncoming laser pulse [1], and such motion already allows PIC modeling. As a result, the high-frequency radiated fields in the far field can be calculated by applying Lienard-Wichert potentials from the particle coordinates and pulses stored at each step of PIC modeling. A separate program was written to calculate this radiation.

The characteristics of synchrotron radiation are presented in Fig. 3. The electron emission field as a function of time (Fig. *3a*) at a distance of 10 m from the modeling region along the line of maximum intensity, which makes an angle of -11.2º from the *z-axis*, has the appearance of noise, which is due to the uncorrelated emission of individual mirror electrons having different coordinates and pulses. The duration of the radiation pulse is determined by the transit time of the counter wave along the relativistic mirror and the surrounding electrons (Fig. *2c*). The middle part of the radiation pulse with large amplitudes with a duration of about $1.5T_0$ (at the 1/e level) is formed by the most energetic electrons of the relativistic mirror located near the axis of the laser pulse, while the beginning and the end of the radiation pulse are formed by less energetic electrons surrounding the mirror from both sides. All electrons with energy γ at time $5T_0$, satisfying the condition $\gamma < \gamma_m - 20$, where γ_m is the energy of the most energetic electrons at this time, did not participate in the calculation of the field in the far field.

The counter wave includes only one field period, so the emission of a single electron (particle in PIC modeling) consists of two short pulses (highlighted by the red ellipse in Fig. *3c*), positive and negative, separated by a time interval where the field is small. This time interval is much longer than the duration of the pulses. This structure of electron emission arises because of the different time conversion when the velocity and acceleration of the electron change during its motion in the counter wave field. Where the pulses overlap, an enlarged peak appears. Since the initial density distribution in the target is random, the distances between the emission pulses of different particles also obey a random law (Fig. *3b*), and the total field emitted by all electrons becomes stochastic.

SPECTRAL DENSITY OF THE RADIATION FIELD AND ANGULAR DISTRIBUTION OF THE PULSE ENERGY

The frequency and angular characteristics of the synchrotron emission of the relativistic mirror electrons are shown in Fig. 4. The spectral density of the radiation field at a point at a distance of 10 m from the modeling region along a line making an angle of -11.2° from the *z-axis* for the same amplitude of the counter wave ($a_1 = 1$) are shown in Fig. *4*a. The spectral density was calculated using the Welch algorithm. The spectral field density has a modulation characteristic of synchrotron radiation generation by electrons in the laser wave field [12]. This form of the spectrum contains several smooth maxima, which arise when the spectra of two close in shape positive and negative pulses, which constitute the full pulse of radiation of one electron, are superimposed (Fig. *3c*). The modulation period is determined by the distance between the pulses, and the total width of the spectrum is determined by the pulse duration. The addition of the emission from all electrons leads to additional random high-frequency modulation of the spectrum, since for two electrons in the mirror, the modulation frequency of their joint spectrum is greater the greater the time distance between their emission pulses, resulting in a spectrum that is actually linear (see the first, second, and third maxima in Fig. *4a*). The modulation period is about 1.4-10^{18}Hz, i.e., of the order of 5.8 keV. The maximum value of the spectral density is reached near the frequency of 2-10^{18}Hz, and the photon energy is about 8.3 keV. Nine modulation periods are clearly visible in the spectral density, thus forming incoherent X-ray radiation with a maximum photon energy of more than 50 keV. For other directions, the maximum energy of the emitted photons decreases, and the modulation period of the spectrum also becomes smaller. Thus, at an angle of 9°, 4 maxima with a width of each about

7.5-10^{17}Hz are observed, which corresponds to a maximum photon energy of about 12 keV.

Fig. $4b$ shows the integral (in terms of frequency) energy of the X-ray radiation pulse as a function of the angle from the z-$axis$ at a distance of 10 m from the modeling area. The pulse energy has a maximum at a deviation from the z-$axis$ by an angle of -11.2°, which corresponds to the direction of the velocity of the most energetic electrons at the moment of time corresponding to the middle of the interaction interval of the counter wave with the mirror (Fig. $2b$). The full width of the distribution is of the order of 2° (at the level of half height), which is in good agreement with the maximum energy of electronsγ during the interaction [1]. The polar diagram in Fig. $4c$ demonstrates that a narrow needle beam is formed, which can find use in many applications.

The spectral radiation field density of the electron emission field of the relativistic mirror for the increased amplitude of the counter wave$a_1 = 5$ is shown in Fig. 4г. In this case, the modulation of the spectral density is practically absent because the distance between two pulses entering the field emitted by each electron has increased and the modulation period has become small. The maximum of the spectral density shifted to a frequency of 5-10^{18}Hz, while the photon energy increased 2.5 times to the value~ 20.7 keV. At the same time, the maximum value of the spectral density increased insignificantly (approximately by 30%), and its width increased more than 2 times, so that the maximum photon energy appeared to be more than 100 keV.

The integral (on the spectrum) energy of the X-ray pulse as a function of angle for the increased amplitude of the counter wave is shown in Fig. 4д. The width of the distribution remained practically unchanged, which is due to the presence of the accelerating laser pulse field during the interaction of the mirror electrons with the counter wave. At the same time, the maximum energy in the pulse increased by a factor of 2.6 in accordance with the broadening of the spectrum of the generated radiation.

DISCUSSION OF RESULTS

The maximum energy of electrons of the relativistic mirror$\gamma_{max} = 2a_0^2 = 200$ is achieved for the acceleration time$T_{acc}/T_0 \approx 3a_0^2/8 = 75$ at the chosen parameters of the accelerating pulse and target [3,4]. Therefore, a simple delay of the counter wave can be used to control the energy of the accelerated electrons during the interaction. By choosing the maximum delay, it is possible to obtain photon energies up to almost 1 MeV. Increasing the amplitude of the accelerating pulse will also increase the energy of the emitted photons even at small acceleration times. Thus, for$a_0 = 20$ the energy of electrons increases four times, and the maximum energy of photons 16 times, i.e. gamma rays can already be generated. Another possibility to control the photon energy is to increase the amplitude of the counter wave. Since the angular distribution of radiation with increasing the amplitude of the counter wave changes weakly (at at least up to the value$a_1 = 5$), the energy efficiency of the scheme in experimental applications can be increased by choosing comparable amplitudes of the accelerating and counter waves and optimal delays of the counter wave relative to the accelerating one. Simultaneously with the increase of the maximum photon energy, the energy in the emitted pulse also increases.

Another important characteristic of X-ray radiation is the pulse duration. In the computational experiment, the pulse duration was determined by the transit time of the counterwave through the mirror and was of the order of 5 fs, with a mirror diameter of about 10 μm (the region where accelerated electrons with high energy are located). The pulse duration can be reduced by choosing an accelerating pulse with a smaller diameter (which will also relax the laser power requirements), or by reducing the diameter of the counter wave (when using a counter pulse with a Gaussian transverse distribution in the experiments). Estimates show [6] that in this case the X-ray pulse duration can be several hundred attoseconds. In addition, focusing of the counterwave also makes it possible to reduce the diameter of the X-ray source to a size of the order of 1-2 μm.

Thus, the advantages of the scheme are: the possibility to control the parameters of the formed pulse; attosecond duration of the generated X-ray and gamma radiation; minimum source diameter of the order of 1-2 μm; width of the formed beam of 1-2 degrees and less than (needle beam); possibility to form simultaneously at different angles time-synchronized pulses with different photon energies.

Plants with these characteristics can be used successfully in many applications.

CONCLUSION

Thus, the generation of X-rays in the interaction of a counter laser wave with a relativistic electron mirror formed by a powerful accelerating laser pulse from a plasma layer has been investigated using computational experimental methods. The fields emitted by electrons in the far-field zone can be calculated by applying the Lienard-Wichert potentials using the coordinates and impulses of particles stored at each step of PIC modeling. The structure of the radiated field in the far field is investigated, the spectral density of the radiation field and the angular distribution of the momentum energy are found. It is shown that for the accelerating field with the amplitude $a_0 = 10$ the maximum energy of X-ray photons is more than 50 keV for the counter wave with the amplitude $a_1 = 1$ and more than 100 keV for $a_1 = 5$, and the angular distribution has a full width of about 2 degrees, i.e. a narrowly directed (needle) beam is formed. Changing the amplitudes of the accelerating and counter wave allows changing the maximum energy of the emitted photons and the energy in the radiation pulse, which makes it possible to create a fully optical X-ray source with controlled parameters.

REFERENCES

1. *Corde S., Phuoc K.T., Lambert G. et al.* // Rev. Mod. Phys. 2013. V. 85. No 1. P. 1.
2. *Kulagin V.V., Cherepenin V.A., Hur M.S. et al.* // Phys. Rev. Lett. 2007. V. 99. Art. No. 124801.
3. *Kulagin V.V., Cherepenin V.A., Gulyaev Y.V. et al.* // Phys. Rev. E. 2009. V. 80. Art. No. 016404.
4. *Kulagin V.V., Kornienko V.N., Cherepenin V.A. et al.* // Quantum. Electron. 2013. V. 43. No. 5. P. 443.
5. *Kulagin V.V., Kornienko V.N., Cherepenin V.A.* // Quantum. Electron. 2016. V. 46. No. 4. P. 315.
6. *Kulagin, V.V.; Kornienko, V.N.; Cherepenin, V.A.* // Zhurn. radioelectron. 2015. № 12. C. 1.
7. *Martinez B., d'Humières E., Gremillet L.* // Phys. Rev. Research. 2020. V. 2. Art. No. 043341.
8. *Dromey B., Cousens S., Rykovanov S. et al.* // New J. Phys. Phys. 2013. V. 15. Art. No. 015025.
9. *Li H.Z., Yu T.P., Hu L.X. et al.* // Opt. Express. 2017. V. 25. N. 18. P. 21583.
10. *Shen X., Pukhov A., Qiao B.* // Commun. Phys. 2024. V. 7. P. 84.

11. *Andreev, A.A.; Platonov, K.Y.* // Quant. electron. 2022. T. 52. № 2. C. 195; *Andreev A.A., Platonov K.Yu.* // Quantum Electron. 2022. V. 52. No. 2. P. 195.
12. *Lee K., Cha Y.H., Shin M.S. et al.* // Phys. Rev. E. 2003. V. 67. No 4. Art. No. 026502.

FIGURE CAPTIONS

Fig. 1. Characteristics of the relativistic mirror electrons after 4.5 periodsT_0 of the laser field from the beginning of the simulation: spatial distribution of electrons (a), longitudinal pulse (red curve 1) and normalized energyγ (blue curve 2) (b), transverse pulse (c). The impulses are normalized by *m s*.

Fig. 2. Characteristics of the most energetic electrons of the relativistic mirror as a function of time: normalized energyγ (blue curve) and longitudinal momentum $p_{(z)}$ (red curve) (a), normalized transverse momentum $p_{(x)}$ (blue curve) and angle of the velocity vector (in degrees) with respect to the *z-axis* (red curve) (b), geometry of interaction of the relativistic electron mirror with the counter wave at the moment of time $4.5T_0$ from the beginning of the simulation (the counter wave is schematically shown by the blue bar, in the figure the scales along the *z* and *x* axes are different) (c).

Fig. 3. Characteristics of synchrotron radiation: time dependence of the electron emission field at a distance of 10 m from the modeling area along the line of maximum intensity, which makes an angle of -11.2° from the *z-axis* (a); the electron emission field in an enlarged scale (b); pulses of single electron emission (c). Here and below,

the field $E_y$is presented in relative units, time t in seconds). The red ellipse in Fig. *3c* shows the emission pulse of a single electron.

Fig. 4. Frequency and angular characteristics of synchrotron radiation of electrons of a relativistic mirror: spectral density of the radiation field at a point at a distance of 10 m from the modeling area along the line making an angle of -11.2º from the *z-axis* (a) (here and below the spectral density is presented in relative units); integral (over the spectrum) energy of the X-ray radiation pulse as a function of the angle from the *z-axis* at a distance of 10 m from the modeling area (b); the same, but in polar coordinates (c), spectral density of the radiation field for the increased amplitude of the counter wave$a_1 = 5$ (d); integral (by spectrum) energy of the X-ray radiation pulse depending on the angle for the increased amplitude of the counter wave (e).

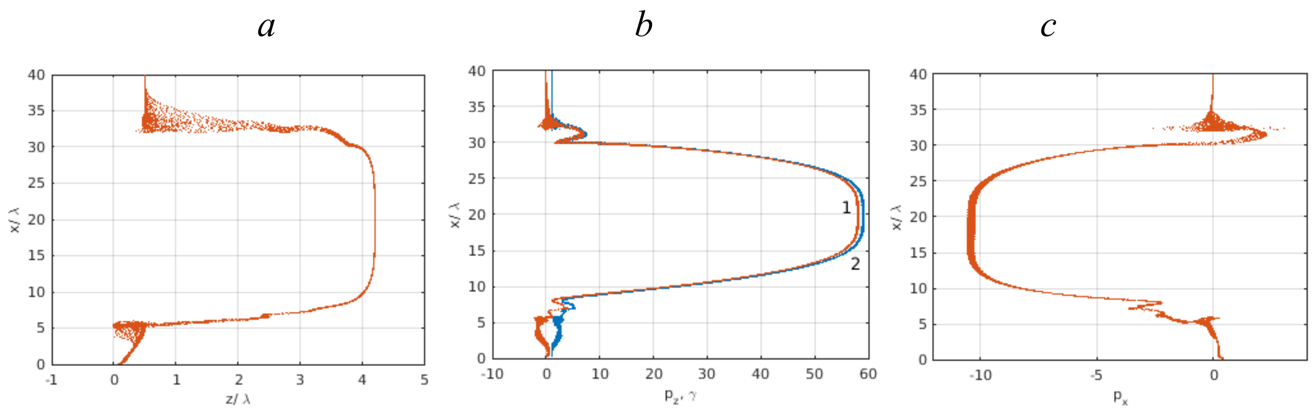

Fig. 1.

a *b* *c*

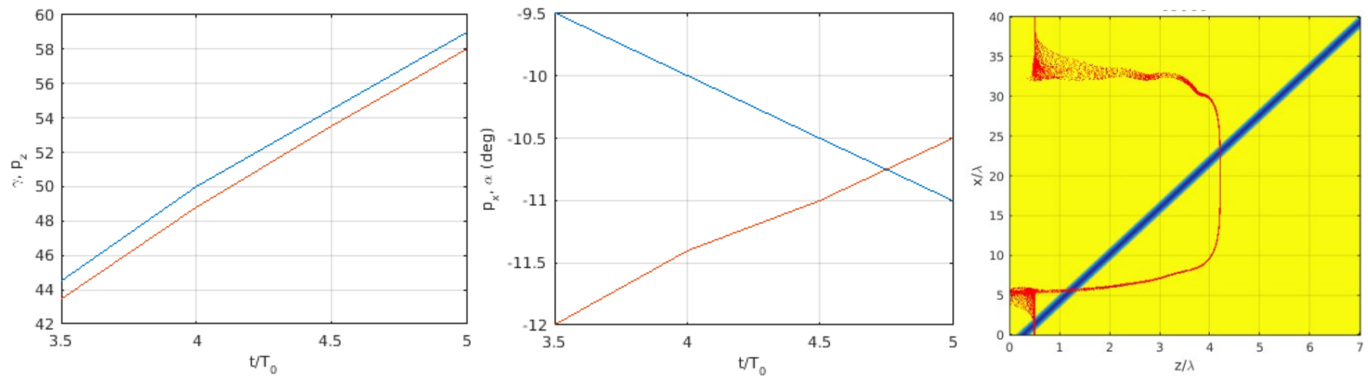

Fig. 2.

a *b* *c*

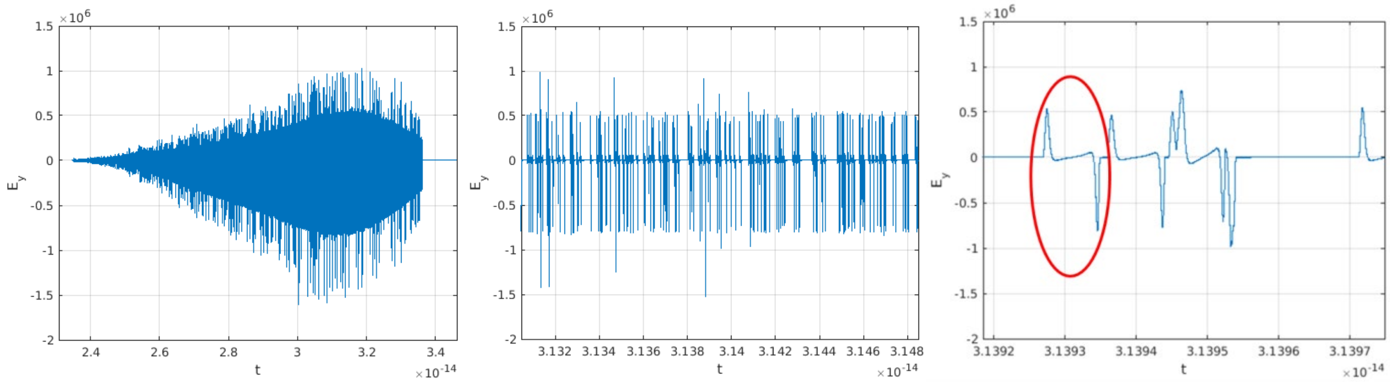

Fig. 3.

a *b* *c*

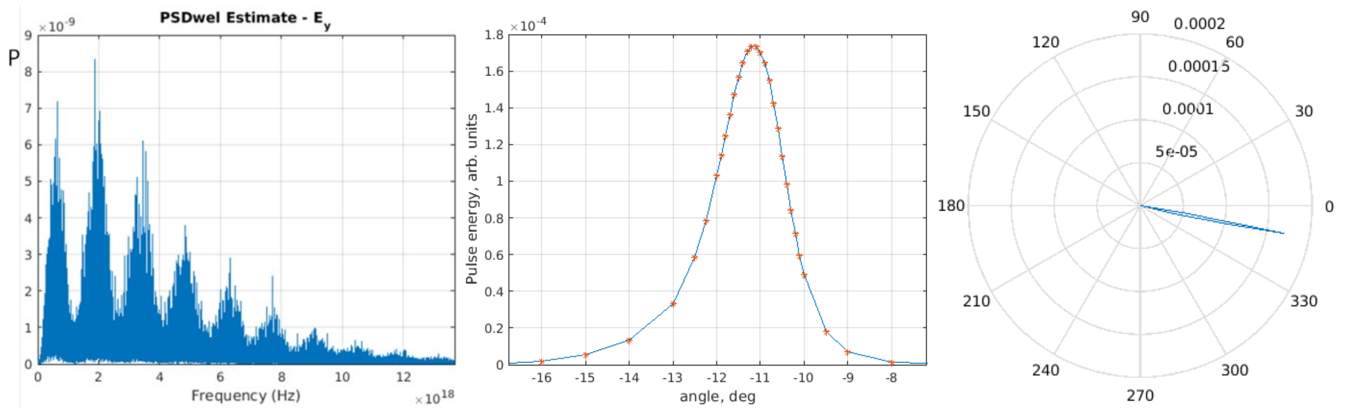

d *e*

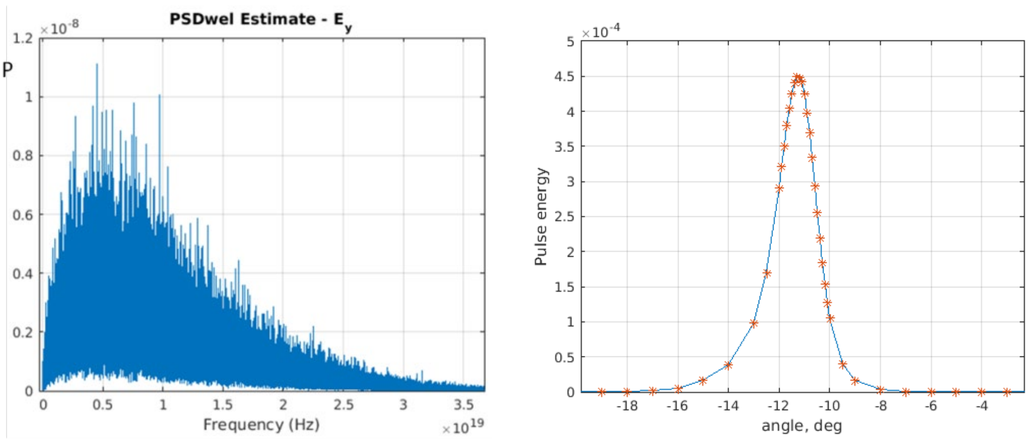

Fig. 4.